中國機械工程學刊第四十卷第六期第 655~661 頁(民國一百零八年)
Journal of the Chinese Society of Mechanical Engineers, Vol.40, No.6, pp 655~661 (2019)

# $TiO_2$ and $CeO_2$ with SS316 Electrode for Degradation of Rh B in Photoelectric-Fenton System

Yi-Ta Wang *, Cheng-Ying Xie**, Yue-Sheng Lin**, Chaur-Jeng Wang***

**Keywords**：Photocatalyst, Rh B, $TiO_2$, $CeO_2$, Photoelectric-Fenton

## ABSTRACT

In this research, photoelectric-Fenton reaction (advanced oxidation program) and photocatalysis were combined for treating Rh B wastewater. A certain percentage of $CeO_2$ added into $TiO_2$ after calcination can improve the effect of degradation. The composite ($TiO_2$-$CeO_2$) was used to modify the stainless-steel material (SS316). The results showed that the porosity of the plate after optimal parameterization was 18%, indicating that the electrode can effectively increase the contact area of the composite $TiO_2$-$CeO_2$, increasing its response current 2.11 times in linear sweep voltammetry. The conductivity of the modified electrode was 1.88 times greater than that of SS316 in a four-point probe experiment. In the Tafel corrosion experiment, the plate after optimal parameterization had a corrosion potential ranging from -299 mV to -160 mV and a corrosion current ranging from 524 nA to 107 nA, which greatly improved the anticorrosion effect of the original SS316 substrate. In the photoelectric-Fenton experiment, the degradation rate of the composite electrode was 50.83% in 30 min, which was 1.26 times higher that of the SS316 substrate. The results showed that the 3 $TiO_2$: 1 $CeO_2$:/SS316 electrode has good stability and a good degradation effect in the Photoelectric Fenton process.

## INTRODUCTION

In recent years, the rapid development of industry has caused increasingly serious pollution. An advanced oxidation process (AOP) has the advantages of low cost and high efficiency compared to other sewage treatment methods; therefore, it has gradually emerged as the new mainstream method to treat sewage in recent years (Babuponnusami, 2012).

The traditional Fenton system produces ferric ions ($Fe^{3+}$) during the reaction process, and it forms precipitates to generate the sludge. The sludge increases the cost of manual treatment and the maintenance time (Gumus, 2016). The photoelectric Fenton is a kind of AOP, it can convert a ferrous ion ($Fe^{2+}$) in the reaction process into a ferric ion ($Fe^{3+}$) by external voltage, and it can produce a cyclic reaction to maintain the system with itself. The reaction is described and expressed by Equations (1) – (3). The oxidation and reduction rates of ferrous ions and hydrogen peroxide ($H_2O_2$) can be increased under ultraviolet (UV) light irradiation, thereby increasing the rate of formation of hydroxyl radicals (·OH). Babuponnusami compared the degradation rate of phenol wastewater by Fenton, electro-Fenton, sono-electro-Fenton, and photoelectric-Fenton processes. The result shows that the rate constant value of photoelectric-Fenton was 0.0934 $min^{-1}$, which was 3.26 times higher than that of the electro-Fenton process (Babuponnusami, 2012). The reaction can be described and expressed by Equations (4) and (5) (Liu, 2018).

$$2H^+ + 2e^- + O_2 \rightarrow H_2O_2, \tag{1}$$

$$Fe^{2+} + H_2O_2 \rightarrow Fe^{3+} + \cdot OH + OH, \tag{2}$$

$$Fe^{3+} + e^- \rightarrow Fe^{2+}, \tag{3}$$

$$H_2O_2 + UV \rightarrow 2OH, \tag{4}$$

$$Fe\,(OH)^{2+} + UV \rightarrow Fe^{2+} + OH, \tag{5}$$

The principle of the photocatalyst is that, when the atom of the semiconductor material receives the energy of the UV light to reach a boundary of energy,

*Paper Received November, 2018. Revised February, 2019, Accepted June, 2019, Author for Correspondence: Yi-Ta Wang.*

* *Associate professor, Department of Mechanical and Electro-Mechanical Engineering, National ILan University, Yilan City, Yilan County 26041, Taiwan.*

** *Graduate student, Department of Mechanical Engineering, National Taiwan University of Science and Technology, Daan District, Taipei City 10607, Taiwan.*

******* *Professor, Department of Mechanical Engineering, National Taiwan University of Science and Technology, Daan District, Taipei City 10607, Taiwan.*

it transitions from the valence band to the conduction band to generate a positively charged hole. The hole reacts with water molecules to produce hydroxyl radicals and $H_2O_2$. The $H_2O_2$ facilitates the acceleration of the photoelectric-Fenton reaction. The photocatalyst reaction is described and expressed by Equations (6)–(12) (Zhang, 2013).

$$TiO_2+HV\rightarrow TiO_2(e^-+h^+), \qquad (6)$$
$$TiO_2(h^+)+H_2O_{ads}\rightarrow TiO_2+OH\cdot_{ads}+H^+, \qquad (7)$$
$$TiO_2(h^+)+OH^-\rightarrow TiO_2+OH\cdot_{ads}, \qquad (8)$$
$$TiO_2(e^-)+O_2\rightarrow TiO_2+O_2\cdot^-, \qquad (9)$$
$$O_2\cdot^-+H_2O\rightarrow OH_2\cdot+OH^-, \qquad (10)$$
$$2OH_2\cdot\rightarrow H_2O_2+O_2, \qquad (11)$$
$$TiO_2(e^-)+H_2O_2\rightarrow TiO_2+OH^-+OH\cdot, \qquad (12)$$

Electrodes are the most important parameter for performance during system operation. An excellent electrode should possess high specific surface area, electrical conductivity, corrosion resistance, and stability (Huggins, 2014). Nidheesh (2012) pointed out that, for the metal, stainless steel has high potential in AOP because of its chemical stability and corrosion resistance. Chou et al. (1999) used stainless steel, graphite, titanium, and lead as an electrode. The result showed that stainless steel has the best property for a reaction of ferrous ions ($Fe^{3+}/Fe^{2+}$), and it can promote the AOP with a stable reaction These studies indicated that stainless steel is suitable to use in the AOP.

Titanium dioxide ($TiO_2$) is the common material in photocatalytic processes, because of its low cost and high oxidation. In addition, the anatase type of $TiO_2$ enhances the anticorrosion property (Abdullah, 2015). The properties of $TiO_2$ can be strengthened by a composite with another material. Deng pointed out that cerium oxide ($CeO_2$) not only can effectively increase the electrochemical properties of the surface area and the conductivity of $TiO_2$, but it also can reduce the bandgap of $TiO_2$ to improve the efficiency of wastewater degradation (Deng, 2018). Wang et al. (2010) formed a composite of cerium (Ⅳ) oxide ($CeO_2$), tin oxide ($SnO_2$), and zirconium oxide ($ZrO_2$) with $TiO_2$. The result showed that, when $CeO_2$ is used to modify $TiO_2$, the Acid Red B can be degraded to 85%, which a better result than those of the others.

In this study, SS316 stainless steel was used as the substrate, and a certain percentage of $CeO_2$ was used for a composite with $TiO_2$. Then, it was coated on SS316 to enhance the electrochemical and photocatalytic ($CeO_2/TiO_2$/SS316) properties and improve the efficiency of wastewater treatment further.

## MATERIALS AND METHODS

The principle of the AOP is that the $H_2O_2$ is generated with the operating voltage in the cathode system, and the $H_2O_2$ reacts with the ferrous ions ($Fe^{2+}$) in the solution to form the Fenton reaction and produce the hydroxyl radical (·OH), which can make the wastewater convert to $CO_2$ and $H_2O$ (Do, 2017). In this study, a $CeO_2/TiO_2$/SS316 electrode was prepared to evaluate the efficiency of the electrode in the AOP. The procedure of the experiment is listed in this section, and the experiments were conducted to analyze the influences between the electrochemical and electrical conductivity properties.

### 1. Cathode preparation

### 1.1. Substrate pretreatment

In this study, SS316 stainless steel (the chemical composition is shown in Table 1) with excellent electrical conductivity and good electrochemical properties was used as the cathode substrate (Ozcan, 2018). The material was cut into 80 (L) × 25 (W) × 2 (H) mm by laser cutting, and the surface was ground with #100 water sandpaper. Then, the substrate was cleaned by shaking with an ultrasonic oscillating machine in ethanol for 30 min.

Table 1. Chemical composition (%) for SS316 stainless steel in this study

| C | Si | Mn | P | S | Ni | Cr | Mo | N | Cu |
|---|---|---|---|---|---|---|---|---|---|
| 0.013 | 0.6 | 0.6 | 0.05 | 0.001 | 10 | 16.64 | 2.05 | 0.01 | 0.32 |

### 1.2. Powder preparation

In this study, 3 mol of $TiO_2$ (Japanese reagent, Japan) and 1 mol of $CeO_2$ (Japanese reagent, Japan) were mixed with ethanol, and the ultrasonic stirrer was shaken for 30 min to thoroughly mix the powder. The solution was sent to a calciner, and the temperature was raised to 450 °C at a rate of 5 °C/min. The temperature was maintained for 2 h. Finally, the powder was prepared cooled to room temperature.

### 1.3. Cathode preparation

The coating was prepared by using N-methyl pyrrolidone as a solvent and adding polyvinylidene difluoride (PVDF). First, the solution was heated to 80 °C with a magnetic stirrer and stirred for 30 min. Different proportions of $TiO_2$ and $CeO_2$ powders were then mixed (the configuration is shown in Table 2). An ultrasonic oscillating machine was used to make the slurry. After the solution was shaken with powder and solvent for 30 min, the slurry was applied to the surface of the SS316 stainless-steel substrate and then heated to 100 °C. When the plate was dry, the electrode was placed in a vacuum oven and heated to 160 °C for 6 h, and the electrode fabrication was completed.

Table 2. Experimental designs for surface modification of SS316 electrode in this study

| **Experimental configuration** | **1** | **2** | **3** |
|---|---|---|---|
| **Total** | 4 mol | 4 mol | 4 mol |
| **$CeO_2$** | 4 mol | 0 mol | 3 mol |
| **$TiO_2$** | 0 mol | 4 mol | 1 mol |
| **Electrode** | $CeO_2$ /SS316 | $TiO_2$ /SS316 | $CeO_2$/ $TiO_2$ /SS316 |

## 2. Analytical method

### 2.1. Porosity analysis experiment

In this experiment, each test group was treated with a gold-plating machine. Surface photography at 10,000-times magnification was performed by scanning electron microscope (SEM). The surface porosity analysis was performed by analysis with the Image J software.

### 2.2. Four-point probe experiment

To test the resistance of the electrode, a four-point probe station (SRS4000, Jiehan, Taiwan) was adapted to measure its sheet resistance. To ensure the accuracy of the result, all the electrodes were measured for three positions, and the result was obtained after averaging.

The impedance of the electrode was measured by applying two currents to the surface, and the potential difference between two ends was calculated by the other two probes to obtain a sheet resistance value for the electrode — the unit is ohm-meter ($\Omega \cdot \mathrm{m}$). The conductivity ($\sigma$) is the reciprocal of the resistivity, as shown in Equation (13). That serves as the basis for judging the conductivity of the material. The unit is 1/ohm-meter — $1/(\Omega \cdot \mathrm{m})$ — equivalent to siemens/meter (S/m).

$$\sigma = \frac{1}{\rho} \ . \tag{13}$$

### 2.3 Electrochemical linear sweep voltammetry measurement

Linear sweep voltammetry (LSV) can be used to evaluate the ability to generate $H_2O_2$ by a working electrode — the scan range was between 0 and −1 V in this study (Wei, 2018).

In this experiment, 200 ml of 0.1M $KNO_3$ solution was dispensed, and the pH value of the solution was adjusted to the optimal parameter pH 3 (Liu, 2018). Then, the reference electrode, counter electrode, and working electrode were equipped to form the experimental condition. The solution was measured in oxygen for 15 min by a flow meter.

### 2.4. Tafel corrosion test

In this experiment, the Tafel curve was measured to test the corrosion characteristics of the electrode. The cathode electrode was used as the working electrode, saturated calomel (Ag/AgCl/KCl) was used as the reference electrode, and platinum was used as the counter electrode.

After the open-circuit voltage was scanned, the corrosion potential and corrosion current of the cathode electrode in the solution were observed by the potentiodynamic method (Panahi, 2018), and then the corrosion potential and current were calculated by interpolation. The corrosion resistance effect of the electrode with surface modification and the substrate was found.

### 2.5. Experiment of degradation of Rh B wastewater by photoelectric-Fenton system

The photoelectric-Fenton system is an AOP. In this study, 200 ml of solution with 0.1-M $KNO_3$ and 20 ppm of ferrous ion was used, and 20 ppm of Rh B solution was added as a regent. The pH value of the solution was adjusted to 3 (Wei, 2018). The reference electrode, counter electrode, working electrode, and quartz tube were used for the system setup. After standing for 15 min with an aeration device, the electrochemical workstation was discharged at a constant voltage of -0.9 V, and a UV lamp was turned on. The degradation rate was measured by spectrophotometry every 3 min to analyze the degradation efficiency of the working electrode.

## Results and discussion

### 3.1. Porosity analysis experiment

You et al. (2016) found that conductivity, specific surface area, contact angle, and corrosion resistance were notably affected by porosity. Deng et al. (2018) also pointed out that the addition of $CeO_2$ to $TiO_2$ can effectively increase the surface area after calcination. The surface porosity with $CeO_2$/SS316, $TiO_2$/SS316, and $CeO_2$/$TiO_2$/SS316 is shown in Figures 1-3.

This result showed that the porosity was 18.33% with the use of composite $TiO_2$ and $CeO_2$ powders for the modified electrode. That is much higher than the porosity of 8.88% when modified by $TiO_2$. Because of the characteristics of $CeO_2$, the porosity of the cathode modified with $CeO_2$ was 5.81%. This result is also consistent with the description provided by Zhang (Zhang, 2008). The values of surface porosity for $CeO_2$/SS316, $TiO_2$/SS316, and $CeO_2$/$TiO_2$/SS316 are shown in Table 3.

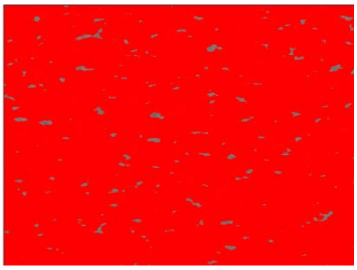

Fig. 1. Figure of the surface porosity for $CeO_2$/SS316

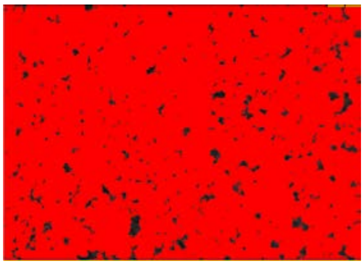

Fig. 2. Figure of the surface porosity for $TiO_2$/SS316

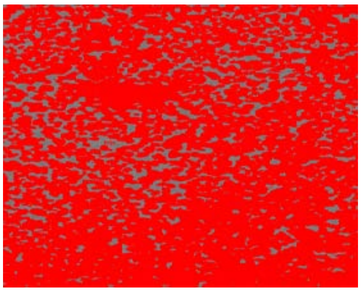

Fig. 3. Figure of the surface porosity for $CeO_2$/$TiO_2$/SS316

Table 3. Surface porosity for $CeO_2$/SS316, $TiO_2$/SS316, and $CeO_2$/$TiO_2$/SS316

| **Electrode** | **$CeO_2$ /SS316** | **$TiO_2$ /SS316** | **$CeO_2$/$TiO_2$ /SS316** |
|---|---|---|---|
| **Surface porosity (%)** | 2.181 | 8.879 | 18.358 |

### 3.2. Four-point probe experiment

Conductivity is an important index of the cathode in the photoelectric Fenton system. The sheet resistance of the polar version was measured by a four-point probe. The sheet resistance is shown in Table 4, and the conductivity is shown in Table 5.

Table 5 shows that the conductivity of the electrode modified by $TiO_2$ and $CeO_2$ composite powder was 1.89 times higher than that of the SS316 substrate. That confirmed that the conductivity of the modified electrode can be effectively improved.

Table 4. Sheet resistance with SS316, $CeO_2$/SS316, $TiO_2$/SS316, and $CeO_2$/$TiO_2$/SS316

| **Electrode** | **SS316** | **$CeO_2$ /SS316** | **$TiO_2$ /SS316** | **$CeO_2$/$TiO_2$ /SS316** |
|---|---|---|---|---|
| **Sheet resistance (Ω • m)** | $4.76*10^{7}$ | $3.10*10^{8}$ | $7.75*10^{7}$ | $2.52*10^{7}$ |

Table 5. Conductivity with SS316, $CeO_2$/SS316, $TiO_2$/SS316, and $CeO_2$/$TiO_2$/SS316

| **Electrode** | **SS316** | **$CeO_2$ /SS316** | **$TiO_2$ /SS316** | **$CeO_2$/$TiO_2$ /SS316** |
|---|---|---|---|---|
| **Conductivity (S/m)** | $2.10*10^{-8}$ | $3.22*10^{-9}$ | $1.29*10^{-8}$ | $3.96*10^{-8}$ |

### 3.3. Linear Sweep Voltammetry

LSV can be used to evaluate the ability to produce $H_2O_2$ in the cathode (Wei, 2018).

In this study, the cathode was analyzed with a working voltage of -0.9 V with LSV. Because the electrode of SS3116 stainless steel had the best $H_2O_2$ production rate at a -0.9-V working voltage, -0.9 V was used as the working voltage of each electrode, and the electrochemical characteristics were compared by using the response current. The LSV curves are shown in Figure 4.

The response current of the cathode modified with $TiO_2$ was 0.9 mA, as shown in Figure 4. That was significantly lower than the response current of the SS316 stainless-steel substrate of 1.15 mA, because the conductivity of $TiO_2$ is poor. This result is consistent with that described by Liu (Liu, 2018). The electrode modified by $CeO_2$ had a lower specific surface area due to its lower porosity, so its response current at an operating voltage of -0.9 V was 0.5 mA. This was significantly lower than those of the other electrodes. This means that the electrode modified with $CeO_2$ had the lowest electrochemical activity.

The cathode of the composite $TiO_2$ and $CeO_2$ had an optimal response current of 2.5 mA at a working potential of -0.9 V. Deng et al. (2018) pointed out that the addition of $CeO_2$ can effectively improve the specific surface area of $TiO_2$ . In addition, the $CeO_2$ has the characteristic of adsorbing oxygen atoms, so its ability to generate $H_2O_2$ is significantly enhanced, and that improves the reaction in the Fenton system.

The $H_2O_2$ generating the current of SS316, $CeO_2$/SS316, $TiO_2$/SS316, and $CeO_2$/$TiO_2$/SS316 at an operating voltage of -0.9 V is shown in Table 6.

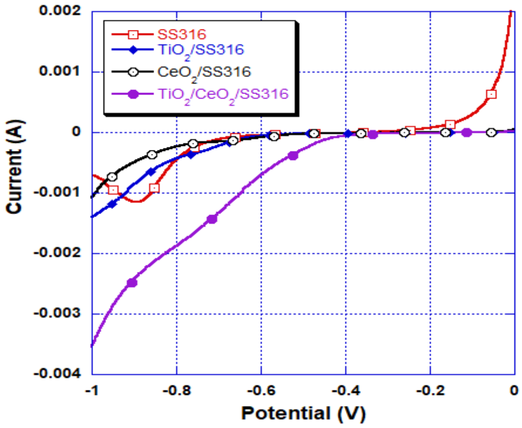

Fig. 4. Curve with SS316, $CeO_2$/SS316, $TiO_2$/SS316, and $CeO_2$/$TiO_2$/SS316 in linear sweep voltammetry

Table 6. Response current of SS316, $CeO_2$/SS316, $TiO_2$/SS316, and $CeO_2$/$TiO_2$/SS316 at an operating voltage of -0.9 V

| Electrode | SS316 | $CeO_2$ /SS316 | $TiO_2$ /SS316 | $CeO_2$/$TiO_2$ /SS316 |
|---|---|---|---|---|
| **Generating current (mA)** | 1.15 | 0.5 | 0.9 | 2.5 |

## 3.4. Tafel corrosion test

Zhongming et al. (2017) pointed out that the corrosion current of the Tafel corrosion experiment affects the corrosion rate of the electrode. When the corrosion current is lower, the corrosion rate decreases. Rekha et al. (2018) also pointed out that the corrosion potential of the Tafel corrosion test affects the electrode, and a higher corrosion voltage indicated that the material can strengthen the corrosion resistance.

In this experiment, the Tafel corrosion test was performed on each electrode after scanning the open-circuit voltage of each electrode. The results show that the $CeO_2$/SS316 electrode obtained the highest corrosion potential of 190.0 mV and a minimum corrosion current of 59.2 nA. In the porosity analysis experiment, the $CeO_2$/SS316 electrode showed the lowest porosity, and the results of this experiment are consistent with the good corrosion resistance of the $CeO_2$ in Zhang's research (Zhang, 2008). The electrode modified by composite $TiO_2$ and $CeO_2$ ($CeO_2$/$TiO_2$/SS316) and the electrode modified with $TiO_2$ ($TiO_2$/SS316) had improved corrosion voltage and corrosion current compared with the -299.0 mV and 807.2 nA of the SS316 stainless-steel substrate. The result showed that the corrosion of SS316 stainless steel can be improved by coating on the surface.

The electrode modified with a composition of $TiO_2$ and $CeO_2$ calcined at 450 °C had the largest promotion. This was because the anatase of $TiO_2$ increased in composite with $CeO_2$. The corrosion voltage rose to -160.0 mV, and the corrosion current was reduced to 107.0 nA. The results of this experiment are consistent with those described elsewhere (Abdullah, 2015). The corrosion voltage V.S. corrosion current of SS316, $CeO_2$/SS316, $TiO_2$/SS316, and $CeO_2$/$TiO_2$/SS316 is shown in Table 7.

Table 7. Value of corrosion voltage V.S. corrosion current of SS316, $CeO_2$/SS316, $TiO_2$/SS316, and $CeO_2$/$TiO_2$/SS316

| Electrode | SS316 | $CeO_2$ /SS316 | $TiO_2$ /SS316 | $CeO_2$/$TiO_2$ /SS316 |
|---|---|---|---|---|
| **Corrosion voltage (mV)** | -299.0 | 190.0 | -220.3 | -160.0 |
| **Corrosion current (nA)** | 807.2 | 59.2 | 715.4 | 107.0 |

## 3.5. Experiment of degradation of Rh B wastewater by photoelectric-Fenton system

Figure 5 shows the degradation rate curves of SS316, $CeO_2$/SS316, $TiO_2$/SS316, and $CeO_2$/$TiO_2$/SS316 degradation of Rh B in a photoelectric-Fenton system after 30 min, indicating that the composite electrode modified with $TiO_2$ and $CeO_2$ can obtain the best efficiency in degrading Rh B.

This has the same trend as an electrode modified with the composite $TiO_2$ and $CeO_2$ powders, which had the best porosity in the porosity analysis experiment, the best conductivity in the four-point probe measurement, and the optimal response current in the LSV. The characteristics of the adsorbed oxygen atom and the specific surface area should be increased, and the photocatalyst energy level decreases after the composite and calcination, improving the electrochemical characteristics, the ability to generate $H_2O_2$, and the efficiency of the Fenton reaction.

The electrochemical degradation rate of the cathode electrode modified by $TiO_2$ was lower than that of the SS316 stainless-steel substrate. However, it compensates for the degradation effect caused by its photocatalytic properties under UV light. The degradation rate was 42.03%, which was superior to the 40.35% of SS316 substrate.

Although the $CeO_2$ possessed the property of adsorbing the oxygen atoms, the electrochemical property of the cathode electrode modified with $CeO_2$ was much lower than that of the other electrodes. Therefore, it degraded the wastewater of Rh B at 34.62% with a poor ability to generate $H_2O_2$. Table 8 lists the degradation rates of Rh B dye wastewater for SS316, $CeO_2$/SS316, $TiO_2$/SS316, and $CeO_2$/$TiO_2$/SS316 after 30 min.

In summary, the cathode modified with the composite $TiO_2$ and $CeO_2$ was applied to the photoelectric-Fenton system, and it had a good reaction efficiency for the photoelectric Fenton system and could effectively degrade the Rh B dye wastewater.

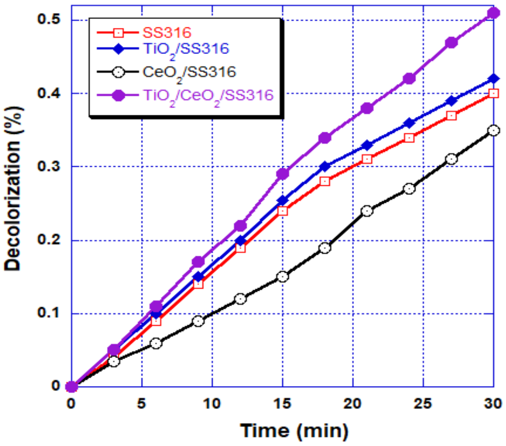

Fig. 5. Degradation rate of SS316, $CeO_2$/SS316, $TiO_2$/SS316, and $CeO_2$/$TiO_2$/SS316 in photo-Fenton

Table 8. Degradation rate of Rh B dye wastewater for SS316, $CeO_2$/SS316, $TiO_2$/SS316, and $CeO_2$/$TiO_2$/SS316 after 30 min

| | **SS316** | **$CeO_2$ /SS316** | **$TiO_2$ /SS316** | **$CeO_2$/$TiO_2$ /SS316** |
|---|---|---|---|---|
| **Degradation rate (%)** | **40.35** | **34.62** | **42.03** | **50.83** |

## Conclusions

The porosity of the plate after optimal parameterization was 18%, indicating that the electrode can effectively increase the contact area when a composite of $TiO_2$ and $CeO_2$ is used, making its response current rise 2.11 times in LSV. The conductivity of the modified electrode was 1.88 times greater than that of SS316 in a modified four-point probe experiment. In the Tafel corrosion experiment, the plate after optimal parameterization had a corrosion potential from -299 to -160 mV and a corrosion current from 524 to 107 nA, which greatly improves the anticorrosion effect of the original SS316 substrate. In the photoelectric-Fenton experiment with the composite plate, the degradation rate was 50.83% in 30 min, 1.26 times that of the SS316 substrate. The results show that the 3 $TiO_2$:1 $CeO_2$:/SS316 electrode has a good stability and degradation effect in the photoelectric Fenton process and indicate that the SS316 modified by the $TiO_2$ and $CeO_2$ composite as the electrode possesses great potential for application in the photocatalyst and photoelectric-Fenton system.

## Acknowledgments

We sincerely appreciate the financial support by the Ministry of Science and Technology, R.O.C. through the grant MOST 106-2221-E-197-018 and supported from laboratory members.

## References

Abdullah, H., Khan, M.R., Pudukudy, M., Yaakob, Z., and Ismail, N.A., “$CeO_2$-$TiO_2$ as a visible light active catalyst for the photoreduction of $CO_2$ to methanol,” J. Rare Earths, Vol. 33, No. 11, pp. 1155-1161 (2015).

Babuponnusami, A., and Muthukumar, K., “Advanced, oxidation of phenol: A comparison between Fenton, electro-Fenton, sono-electro-Fenton and photoelectric-Fenton processes,” Chem. Eng. J., Vol. 183, pp. 1-9 (2012).

Chou, S., Huang, Y.H., Lee, S.N., Huang, G.H., and Huang, C., “Treatment of high strength hexamine-containing wastewater by electro-Fenton method,” Water Res., Vol. 33, pp. 751-759 (1999).

Deng, X., Zhang, H., Guo, R., Cui, Y., Ma, Q., Zhang, X., Cheng, X., Li, B., Xie, M., and Cheng, Q., “Effect of fabricating parameters on photo electrocatalytic performance of $CeO_2$/$TiO_2$ nanotube arrays photoelectrode,” Sep. Purif. Technol., Vol. 193, pp. 264-273 (2018).

Do, T.M., Byun, J.Y., and Kim, S.H., “An electro-Fenton system using magnetite coated metallic foams as cathode for dye degradation,” Catal. Today, Vol. 295, pp. 48-55 (2017).

Gümüş, D., and Akbal, F., “Comparison of Fenton and electro-Fenton processes for oxidation of phenol,” Process Saf. Environ., Vol. 103(A), pp. 252-258 (2016).

Huggins, T., Wang, H., Kearns, J., Jenkins, P., and Ren, Z.J., “Biochar as a sustainable electrode material for electricity production in microbial fuel cells,” Bioresour. Technol., Vol. 157, pp. 114-119 (2014).

Liu, X., Zhou, Y., Zhang, J., Luo, L., Yang, Y., Huang, H., Peng, H., Tang, L., and Mu, Y., “Insight into electro-Fenton and photo-Fenton for the degradation of antibiotics: Mechanism study and research gaps,” Chem. Eng. J., Vol. 347, pp. 379-397 (2018).

Nidheesh, P.V., and Gandhimathi, R, “Trends in electro-Fenton process for water and wastewater treatment: An overview,” Desalination, Vol. 299, pp. 1-15 (2012).

Ozcan, A., Şahin, Y., Koparal, A.S., and Oturan, M.A., “Carbon sponge as a new cathode material for the electro-Fenton process: Comparison with carbon felt cathode and application to degradation of synthetic dye basic blue 3 in aqueous medium," J. Electroanal. Chem., Vol. 616, No. 1, pp. 71-78 (2018).

Panahi, H., Eslami, A., and Golozar, M.A., "Corrosion and stress corrosion cracking initiation of grade 304 and 316 stainless steels in activated Methyl Diethanol Amine (aMDEA) solution," J. Nat. Gas Sci. Eng., Vol. 55, pp. 106-112 (2018).

Rekha, M.Y., Kamboj, A., and Srivastava, C., "Electrochemical behavior of SnNi-graphene oxide composite coatings," Thin Solid Films, Vol. 653, pp.82-92 (2018).

Wang, J., Lv, Y., Zhang, L., Liu, B., Jiang, R., Han, G., Xu, R., and Zhang, X., "Sonocatalytic degradation of organic dyes and comparison of catalytic activities of $CeO_2/TiO_2$, $SnO_2/TiO_2$ and $ZrO_2/TiO_2$ composites under ultrasonic irradiation," Ultrason. Sonochem., Vol. 17, No. 4, pp. 642-648 (2010).

Wei, H., Su, X., Liu, J., Tian, J., Wang, Z., Sun, K., Rui, Z., Yang, W., and Zou, Z., "A $CeO_2$ modified phenylenediamine-based Fe/N/C with enhanced durability/stability as non-precious metal catalyst for oxygen reduction reaction," Electrochem. Commun, Vol. 88, pp. 19-23 (2018).

You, C., Zheng, R., Shu, T., Liu, L., and Liao, S., "High porosity and surface area self-doped carbon derived from polyacrylonitrile as efficient electrocatalyst towards oxygen reduction," J. Power Sources, Vol. 324, pp. 134-141 (2016).

Zhang, W.W., Gong, A.J., Qiu, L., Cao, Y.Q., and Yuan, X.T., "Processes of degradation and removal methods of antibiotics from waste water," Chin. J. Antibiot., Vol. 6, (2013).

Zhang, S., Li, M., Yoon, J.H., Cho, T.Y., Lee, C.G., and He, Y., "The comparative study on microstructure and properties of nano-$CeO_2$ and $Sm_2O_3$ particulate reinforced nickel-based composites by laser deposition," Appl. Surf. Sci., Vol. 254, No. 22, pp. 7446-7452 (2008).

Zhongming, Z., Ying, M., Weiwei, R., Ting, W., Chunjie, X., and Zengzhe, X., "Mechanical Properties and Corrosion Behavior of Hot Extruded $Mg_{99.2}Ca_{0.6}Mn_{0.2}$ Alloy in SBF Solution," Rare Metal Mater. Eng., Vol. 46, No. 9, pp. 2352-2358 (2017).

# 二氧化鈦及二氧化鈰修飾 SS316 電極於光電芬頓場域降解 Rh B 效能探討

王宜達 謝承穎 林岳陞 王朝正
國立宜蘭大學機械與機電工程學系
國立台灣科技大學機械工程學系

## 摘 要

本研究結合光電芬頓（高級氧化程序）和光催化作為處理 Rh B 廢水的方法。在本研究中，煅燒後在二氧化鈦中加入一定比例的二氧化鈰可以提高降解效果。使用複合材料（二氧化鈦-二氧化鈰）後可改良不銹鋼材料（SS316）。結果表明，最佳參數化後之極板其孔隙率為 18％，證實復合 $TiO_2$ 和 $CeO_2$ 後極板可有效提升其接觸面積，使線性掃描伏安法的響應電流上升 2.11 倍。而在四點探針實驗中，修飾後之電極其片電阻較原 SS316 基材降低 1.88 倍。在塔弗腐蝕實驗中，經修飾之極板其腐蝕電位由-299mV 升至-160mV 而其腐蝕電流則由 524nA 降至 107nA 的腐蝕電流，這極大地提高了原 SS316 基板之抗腐蝕效果。而在光電芬頓實驗中，經複合材料修飾之極板其脫色率在 30 分鐘後達 50.83％，為原 SS316 基板的 1.26 倍。結果顯示，3 $TiO_2$：1 $CeO_2$：/ SS316 電極在光電芬頓反應中具有良好的穩定性和脫色效果。